Multiplex droplet assay reveals coinciding inoculum effect and phenotypic heterogeneity during beta-lactam treatment of bacteria

Ott Scheler,[1,2] Pawel R. Debski,[1] Michal Horka,[1] Artur Ruszczak,[1] Natalia Pacocha,[1] Witold Postek,[1] Karol Makuch[1] and Piotr Garstecki[1]

[1]Institute of Physical Chemistry, Polish Academy of Sciences, Kasprzaka 44/52, 01-224 Warsaw, Poland.

[2]Institute of Molecular and Cell Biology, University of Tartu, Riia 23, 51010 Tartu, Estonia

Abstract:

Bacteria population density modulates the effectiveness of antibiotic treatment. Better understanding of the dynamics between bacteria density and antibiotics helps designing improved treatment strategies, and prevent emergence and spread of drug resistance. In here we describe a droplet microfluidic platform designed for parallel analysis of multiple bacteria inoculum densities. We generate a color-coded series of bacteria inoculum densities, split them into 2nL droplets, and pool them together for incubation and analysis. During cefotaxime treatment of bacteria we observed strong inoculum effect, often associated with beta-lactam antibiotics. The technology also revealed two types of phenotypic heterogeneity in our test strain. Firstly, we observed heterogeneity in growth inhibition in samples starting from single bacteria. At sub-inhibitory antibiotic concentrations only a ~10% fraction of bacteria manage to start viable colony in droplet. That hints for a phenotypical differences in molecular mechanisms responsible for reducing effects of beta-lactams. Secondly, we saw intensive clumping of bacteria that is modulated by the inoculum density and antibiotic concentration. The clumping is most intensive at sub-inhibitory concentrations of cefotaxime. Such diversity in population heterogeneity would have been difficult to spot with conventional cytometry or microscopy methods. This demonstrates that the technology we describe here opens up new possibilities in modern microbiology, especially in investigating antibiotic susceptibility and drug resistance.

Introduction/motivation:

In here we demonstrate a droplet microfluidic high-throughput tool for analysis of antibiotic susceptibility and population heterogeneity in virtual array of multiple bacteria densities.

Antimicrobial resistance (AMR) is a global threat as 700 000 people die annually from resistant infections. The number is estimated to rise to 10 million by the year 2050.[1] The exact numbers in the prediction are debatable, but there is no doubt that urgent action is needed to prevent the grim prediction.[2,3] A major cause behind the emergence or drug resistance is ineffective treatment of infections, either by using inappropriate antibiotics or sub-inhibitory concentrations of potentially useful drugs.[4] Better understanding of mechanisms how bacteria manage to overcome antibiotic exposure helps to design better treatment strategies.[5,6] A typical measurement of antibiotic resistance is minimum inhibitory concentration (MIC) of antibiotic that is needed to prevent proliferation of bacteria.[7,8]

A key aspect affecting the antibiotic efficacy and MIC is the density of bacteria population at the start of the treatment as bacteria populations with higher density are often more resilient to antibiotics. This phenomenon is called inoculum effect (IE).[9] IE is mostly associated with beta lactams, but has been show with other types of antibiotics as well.[9–12] The dynamics of antimicrobial susceptibility at different inoculum densities has been investigated by conventional microbiological tools: well-plates,[10,11] turbidostat,[12] agar plate count[13] and animal models.[14] The main disadvantage of traditional methods is that only few inoculum densities are investigated as screening of multiple inoculum densities over wide concentration range requires expensive well-plate handling robot systems.[10]

In here we introduce droplet-based technology[15] for multiplex analysis of different bacteria densities. We use color-coding[16] to mark series of bacteria inoculum densities, split them into 2nL droplets and pool them together for incubation and analysis. We apply our droplet platform to investigate the beta-lactam cefotaxime-associated inoculum effect. More interestingly our technology revealed phenotypic diversity in a) clumping of bacteria during growth and b) growth inhibition at single CFU level.

Results and discussion

[Description of microfluidic technology and color-coding of droplets]

We start by making 16 two-fold dilutions of *Escherichia coli* Dh5α strain that carries plasmid with yellow fluorescent protein (YFP) and second plasmid with TEM-20 weak beta-lactamase gene. First dilution is prepared by refreshing the overnight culture of bacteria in fresh media at 1:10 ratio. Next we label the dilutions of bacteria densities with combination of two fluorescent dyes: Cascade Blue and Alexa 647. We use "virtual array" strategy described by Abate *et al.* in which fluorescent dye combinations are added to bacteria dilutions as 16 different concentration combinations.[16] Both dyes are represented as 4 different concentrations in our virtual array. (Fig 1A) The sample loading and droplet generation has been described previously in details by Scheler *et al*.[17] In brief, the color-coded bacteria samples were introduced to microfluidic tubing from 96-well plate using rotAXYS automated positioning system and programmable neMESYS syringe. Then we aspirated 3 uL of each dilution into microfluidic tubing spaced with equal volume of oil plugs. (Fig 1A).

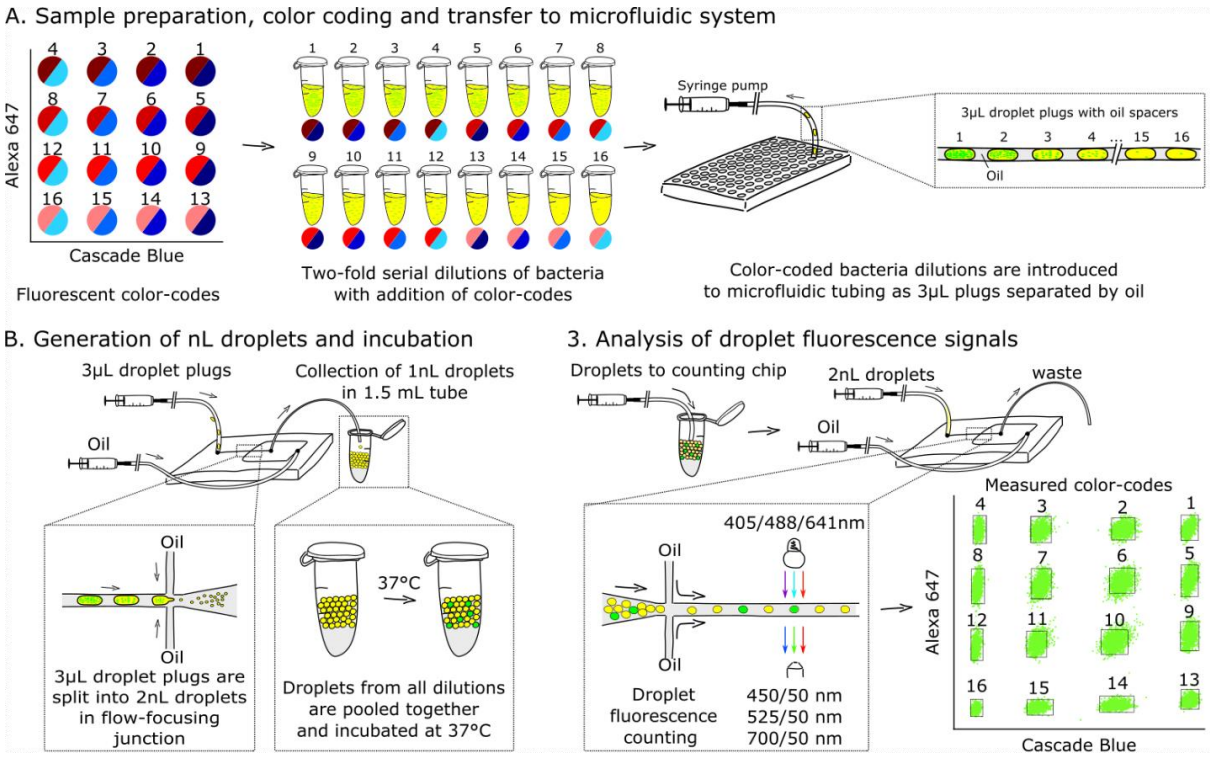

Figure 1 Microfluidic technology and color-coding of bacteria droplets. A) Color-coding of bacteria dilution samples. B) Generation and incubation of 2 nL droplets from color-coded bacteria dilutions. C) Analysis of droplet fluorescence and allocation of droplets according to color-codes

In the next step, we inserted the tubing with dilutions into a poly(dimethylsiloxane) (PDMS) microfluidic chip with a flow-focusing junction (Fig 1B) where we compartmentalized the plugs into ~2 nL droplets (the exact size distribution of droplets is shown in SI-2). Then we collected and pooled the droplets together in a standard 1.5 mL test tube for incubation at 37 °C. (Fig 1B) After incubation, we re-introduced the virtual array to microfluidic tubing and pushed them into the counting chip. Both droplet generation and counting chips had similar flow-focusing geometries (see SI-1 for a precise layout of the

chips). Then, we fixed the chip in a confocal microscope stage to measure the intensity of fluorescence emitted by droplets in three different channels. For spacing the droplets during the measurement, we introduced an additional stream of carrier oil into the flow-focusing junction immediately before the acquisition area. (Fig1C) We use fluorescence intensity levels of Cascade Blue and Alexa 647 to position each droplet in "virtual array" matrix. Then we identify each cluster and determine the bounding box encapsulating the points within and assign color-code number to each gated droplet cluster. The color-coding histogram on Fig 1C shows data from ~22000 droplets (~1400 per each color-coded bacteria dilution). Our virtual array technology allows color-coding more than 97% of droplets in an assay (see SI-3 for further details).

[Inoculum density calculation in droplets]

We calculate initial inoculum density in virtual array (CFU/droplet) by using optimized digital counting algorithm and equations that were described before.[17–19] We set a threshold to distinguish between positive bacteria containing and negative empty droplets in the whole pooled library set based on their relative fluorescence intensity after 22h incubation at 37° C (Fig 2A). Next we investigated dilution libraries separately to calculate positive droplet fractions for each (Fig 2B). After that we used optimized digital algorithms to calculate the average encapsulation event for each library as CFU/droplet (Fig 2C). See SI-4 for more detailed explanation of calculations. The average CFU/droplet ranged from 267 to 0.002. We emphasize that these values show the average of bacteria encapsulation events and the real events always have nonzero natural number values in which 1 is the smallest .

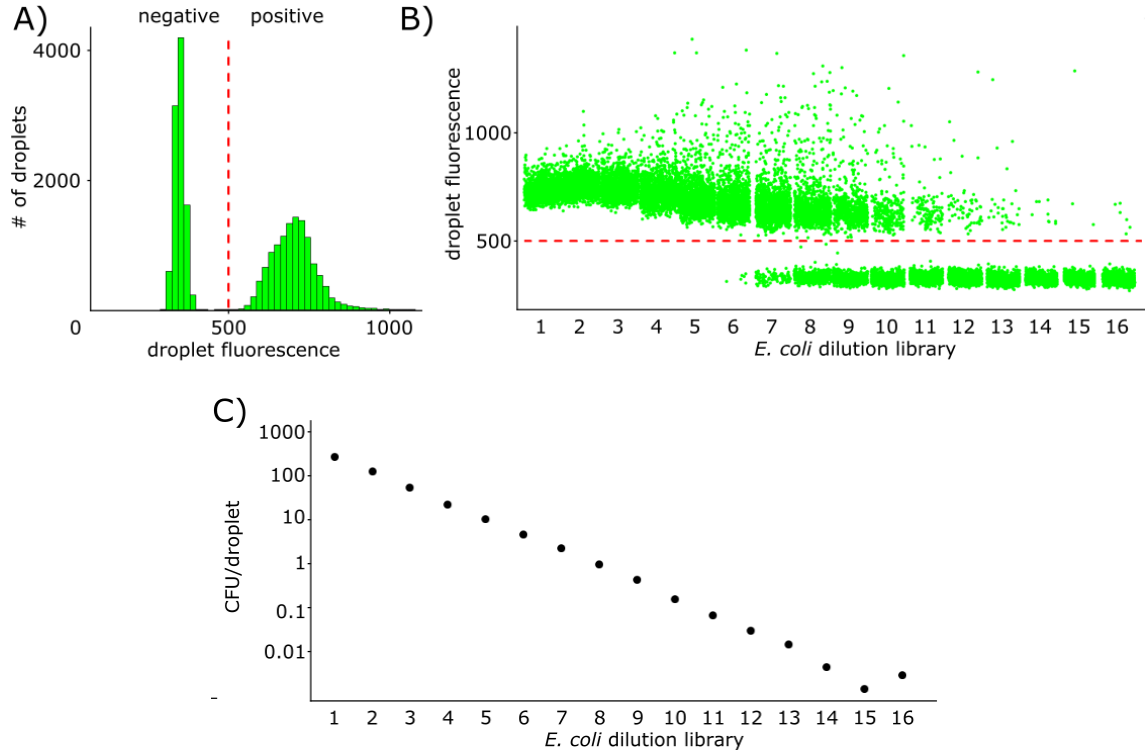

Figure 1 A) A histogram showing the relative droplet fluorescence of negative and positive droplets. Red dashed line represents the set threshold between positive and negative. B) A graph showing the fluorescent intensity of each droplet according to its color-code. C) Average CFU/droplet values for each library

[MIC at different bacteria inoculum densities and inoculum effect]

We investigated the bacteria growth inhibition by beta-lactam antibiotic cefotaxime. This antibiotic works by disrupting the bacterial cell wall synthesis mechanism during cell division.[20] We prepared a two-fold dilution series of 13 cefotaxime concentrations ranging from 0.25 to 1024 µg/mL. Each antibiotic concentration is added to separate virtual array. We use virtual array experiment without antibiotics that we described in previous section as a control to show bacteria growth without antibiotic stress.

For estimating the MIC at each separate bacteria density we plot the fraction of viable bacteria against antibiotic concentrations. The number of viable bacteria is calculated based on initial inoculum density and fraction of droplets demonstrating active bacteria growth at different antibiotic conditions. The MIC curve can be closely approximated using a Gompertz function (reversed sigmoidal function), which is a 3-parameter function.[21,22] The parameters are estimated by means of the least square method. The value of MIC can be estimated as the crossing between the tangent to the Gompertz function in the highest drop and the X axis, which correspond to the logarithm of the concentration of antibiotics (Fig3 A). We note that in this assay we measure the MIC and not the minimum bactericidal concentration (MBC)[7] meaning that bacteria may still be viable after the incubation even if we did not observe the growth in droplets.

We see strong inoculum effect against cefotaxime with *E. coli* Dh5α TEM-20 strain as the MIC increases drastically with higher bacteria densities (Fig3 B). This was predicted as similar findings have been reported with similar bacteria strain.[10] In our case the MIC values were somewhat lower compared to Artemova *et al.* and we credit this to the significantly different experimental conditions that may affect bacteria susceptibility towards antibiotics. We also observed similar IE with different microfluidic setup using smaller droplets and MH growth medium (unpublished data).

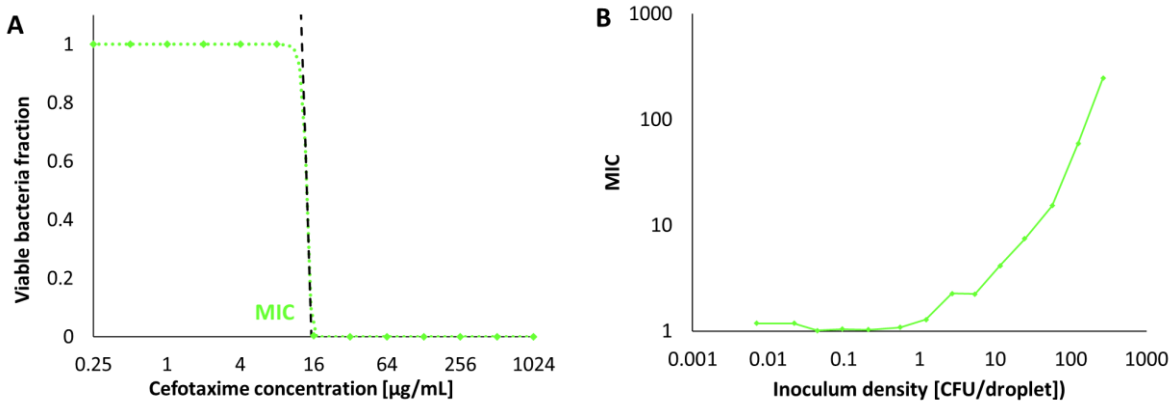

Figure 2 MIC at different bacteria densities. A) calculation of MIC values according to Gompertz function. Experimental data (green dots) is fitted with Gompertz function (green dashed line) and the tangent line (black dashed) to the point of maximum inflection determines the MIC value. Figure shows MIC calculation for average bacteria density of 56.7 CFU/droplet. B) calculated MIC values at different inoculum densities showing the inoculum effect.

[Single cell growth inhibition heterogeneity]

The MIC values below 1 CFU/droplet stay at ~1µg/mL of cefotaxime as the actual bacteria density becomes "locked" at 1CFU/droplet. It shows the robustness of droplet platform for antibiotic susceptibility screening. The exact bacteria density in bulk is not vital in such droplet assay as long as it is below 1 CFU/droplet on average. Preferably, at least as low as 0.1 CFU/droplet to minimize double encapsulation events according to Poisson distribution.[23,24] In that case the compartmentalization guarantees automatically assay conditions for 1 CFU/droplet that in our 2 nL droplets would translate into $5x10^5$ CFU/mL in bulk which is the recommended inoculum density for MIC assays.[8] This makes such droplet platform highly suitable for analysis of bacteria growth starting from single CFU.

In our MIC tests starting from 1CFU/droplet and lower we observed peculiar phenomenon that only a fraction of droplets with bacteria demonstrated uninhibited growth at sub-MIC conditions.(Fig 4) This was not decreased growth rate as the signal intensities in droplets were similar to lower antibiotic concentrations (See SI-8). Emergence of mutants is highly unlikely as the mutation rate in bacteria is orders of magnitude lower than the fraction of survived bacteria in this experiment.[25] They are neither persisters as they grow during constant antibiotic presence.[6] This fraction of growth is also not caused only by double encapsulation in droplets as such high number of double encapsulation events is unlikely. This hints for a phenotypical differences in molecular mechanisms responsible for reducing effects of beta-lactams. The bacteria strain we used in this experiment carries weak beta-lactamase gene TEM-20 in one of its plasmids.[10] High copy-number of that plasmid and stochasticity of its expression could have been behind that heterogeneity. Regardless of the mechanism (genetic of phenotypic) this experiment shows that our droplet platform is suitable for high-throughput screening of heterogeneity in bacteria populations

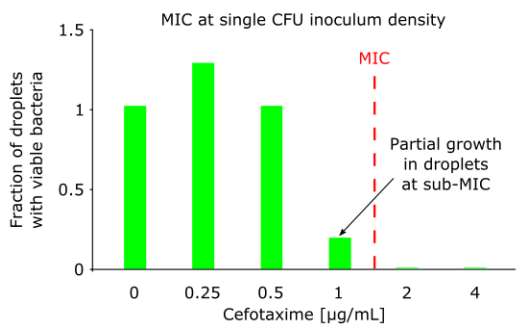

Figure 3 Population heterogeneity at single CFU level. At sub-MIC cefotaxime concentration 1 µg/mL only a fraction of droplets with bacteria demonstrate growth

[Bacteria clumping]

We observed that in some droplets bacteria intensively clump together during growth and this process is modulated by exposure to cefotaxime. First, we noticed clumping in droplets of control "virtual array" without the addition of antibiotics. Clumping is manifested as localization of high intensity pixels in our confocal microscope raw data images (Fig 5A). Then we measured the relative size of bacteria clumps in droplets by dividing the area of clump with droplet area. The clumping was extremely intensive in certain fraction of droplets and this fraction is shown on Fig 5A as top 90 decile of clump sizes in

droplets. In our following analysis we use the 90th decile value (clump size ~1.06%) as a threshold for intensive clumping.

For clumping analysis we included the data from 11 highest densities in virtual array as the lower densities did not have sufficient positive droplets. In control virtual array without antibiotics the clumping starts to increase with bacteria population density until it rapidly drops after 10 CFU/droplet density (Fig 5B). The average size of the clump in the droplet decreases with population density (Fig 5C). The outlier of this trend at the lowest population density is probably artefact due to the small number of clumping events detected.

Next we investigated how clumping is affected by treatment with cefotaxime. For that we re-analyzed the data in our antibiotic susceptibility experiment that was shown in previous section. We applied the same intensive clumping threshold to all virtual arrays with different antibiotic concentrations. Clumping is most extensive near inhibitory concentrations of cefotaxime both in clumping events and the average size of clumps (Fig 5D). The full results of the clumping events and clump sizes in different antibiotic concentrations is shown of Fig 5E and 5D, respectively. We observed similar clumping in smaller droplets using different growth medium (unpublished data).

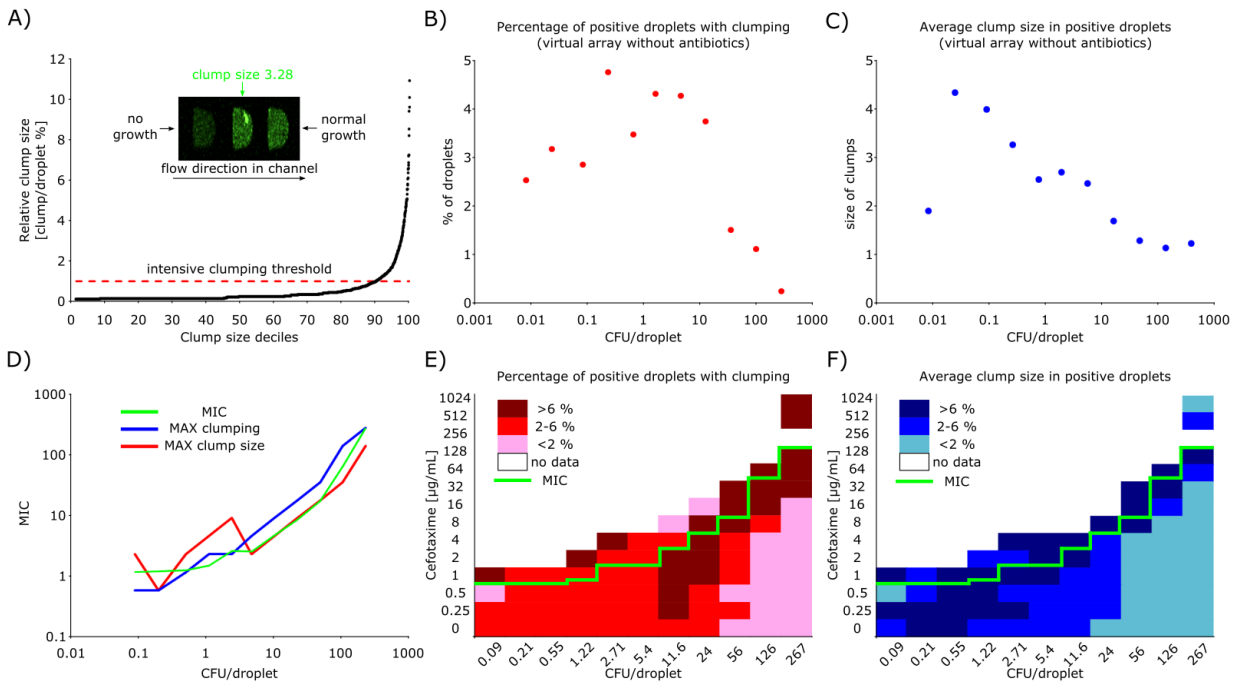

Figure 5 Clumping in droplets. A) Definition of intensive clumping and an example of clumping event in droplet. B) Percentage of positive droplets that demonstrated clumping. C) Average size of clumps in droplets that demonstrated clumping. D) Clumping is most extensive near inhibitory concentrations of cefotaxime E) Clumping events modulation with cefotaxime F) Clump size modulation with cefotaxime

Conclusions:

We demonstrate a new droplet-based technology for versatile analysis of antibiotic susceptibility and population heterogeneity in bacteria. No such thorough analysis of antibiotic induced growth inhibition at different inoculum densities has been done before using droplets. Color-coding of droplets have not been done with bacteria assays before. Clumping analysis has not been done before so thoroughly, probably because lack of suitable technology. Our technology provides simultaneous information about antibiotic susceptibility at different inoculum densities and also population heterogeneity (clumping, single cell inhibition). It is a first demonstration of massively parallel investigation of different phenotypes and heterogeneity in bacteria population during antibiotic growth inhibition. This technology is useful for microbiologists to whom we give a new high-throughput technology that enables i) running multiple microbiological experiments simultaneously and ii) investigate different phenotypes and heterogeneity in bacteria population. For people with microfluidics and engineering background we show how to design multiplex assays for microbiological analysis. The advantage of our technology is that there is no high-throughput technology to screen for different growth phenotypes and population heterogeneity during antibiotic stress (FACS and well-plates show averages of populations). Also, applying color-coding virtual array technology enables pooling together different microbiological droplet assays

The main limiting factor of using droplet technologies for microbial studies is that fluorescence has to be used for labelling bacteria and monitor their growth. However, novel label free concepts are being actively developed for detection and monitoring bacteria activity in droplets.[15] Another concern is that the inoculum density in droplets is limited to 1CFU/droplet which in this project stands for roughly 5x10e5 CFU/mL. In that case, high-throughput uL assays might be needed if lower densities have to be investigated. Droplet microfluidics itself used to be a niche platform for the few designated laboratories, but this has changed recently. Microfluidic chips for generation and handling of droplets are becoming mainstream as the technology for manufacturing them is available to increasing number of research groups. Also, there are several commercial ventures already providing microfluidic chips that are similar to the ones used in this project.

Material and methods:

[Microfluidics]

We used two different microfluidic chips: i) for the generation of droplets and ii) for droplet analysis. Both chips were made of a PDMS fluidic layer that was plasma-bonded to a 1 mm-thick glass slide (see SI-1 for details). The fabrication of the fluidic layer had following steps: i) fabrication of polycarbonate (PC) molds in 5 mm-thick plates of PC (Macroclear, Bayer, Germany) using a CNC milling machine (MSG4025, Ergwind, Poland), ii) we poured PDMS (Sylgard 184, Dow Corning, USA) onto the PC chip and polymerized the mold at 95 °C for 45 min, iii) silanization of the PDMS mold for 3 h under 10 mbar pressure with vapors of tridecafluoro-1,1,2,2-tetrahydrooctyl-1-trichlorosilane (United Chemical Technologies, USA), iv) cleaned PDMS negative masters were employed for molding of the positive PDMS replicas, which we subsequently bonded to a glass slide by exposing both parts for 30 s to oxygen plasma and placing them together, v) we modified the microfluidic channels hydrophobically by filling the chip with Novec 1720 (3M, United States) for 10 min, vi) after fluid evaporation at room temperature, the chips were baked at 135 °C for 1 h to enhance bonding and preserve the modification. We controlled the flow of the oil and reagents in the microfluidic experiments with a rotAXYS

positioning system and neMESYS syringe pumps (both from Cetoni, Germany). Droplets were generated with ~600 Hz frequency and collected for off-chip incubation in 1,5 mL test tubes. We used Novec HFE-7500 fluorocarbon oil (3M, USA) with 2% PFPE–PEG–PFPE surfactant synthesized according to the protocol by Holtze *et al*.[26]

[Microbiology]

In this project we used *E. coli* Dh5α strain that carried two plasmids: i) pBR322 with weak TEM-20 beta-lactamase gene and ii) pZS25O1 with YFP coding-gene. This strain is a kind gift from Prof. Jeff Gore, MIT, USA and has been described before.[10] For bacteria culturing in bulk and droplets, we used LB-Lennox media (Roth, Germany). For plasmid retention we used 50 µg/mL of piperacillin (Sigma-Aldrich, Germany) and 50 µg/mL kanamycin (Thermo Fischer Scientific, USA), and for gene expression induction 1 mM isopropyl β-D-1-thiogalactopyranoside IPTG (Thermo Fisher Scientific). Antibiotic susceptibility tests were carried out with cefotaxime (Sigma-Aldrich).

[Data analysis]

Droplet analysis was carried out similarly to previously described manuscripts with slight modifications.[17,27] We measured the droplet fluorescence in a droplet reading chip that was mounted on the stage of an A1R confocal microscope (Nikon, Japan). For color-coding of droplets in virtual array we used Cascade Blue® 3000MW and Alexa Fluor® 647 10000MW dextran conjugates (both from Invitrogen, USA). We acquired the fluorescence of color-codes at excitation/emission wavelengths of 403.3/425-475 nm and 641.8/663-738 nm, respectively. The YFP fluorescence was acquired at 488/500-550 nm. Raw fluorescence data was analyzed with custom-made LabVIEW scripts (National Instruments, USA). Final analysis was carried out with MS Office Excel (Microsoft, USA) with Real Statistics Resource Pack (www.real-statistics.com) and Peltier Tech Charts 3.0 Add-In (peltiertech.com). Droplet signals stand for the peak relative fluorescence intensities allocated to each droplet at each channel. The MIC distributions were calculated analytically or assessed numerically by means of Monte Carlo simulations. The values of the parameters of the distribution that resembles the recorded output of the experiments were assessed numerically by scanning through all the possible values. The quality of the fit was calculated by calculating the correlation between numerical and experimental data and finding the relation closest to x=y with the highest Pearson correlation factor. All the calculations were carried by means of ROOT mathematical library (root.cern.ch) and C++ macros. See SI for more detailed description about the analysis.

Acknowledgements

This project was supported by National Science Centre funding based on decision number DEC-2014/12/W/NZ6/00454 (Symfonia). This work was supported by the Foundation for Polish Science through the program TEAM TECH/2016-2/10. This work was also supported by the Estonian Research Council grant PUTJD589 (to O. S.).

References:

1 J. O'Neill, *Wellcome Trust UK Gov.*, 2016.

2 G. S. Tillotson, *Lancet Infect. Dis.*, 2017, **17**, 473–474.

3 M. E. A. de Kraker, A. J. Stewardson and S. Harbarth, *PLoS Med.*, 2016, **13**, 1–6.

4 C. L. Ventola, *Pharm. Ther.*, 2015, **40**, 277–83.

5 A. C. Palmer and R. Kishony, *Nat. Rev. Genet.*, 2013, **14**, 243–8.

6 A. Brauner, O. Fridman, O. Gefen and N. Q. Balaban, *Nat. Rev. Microbiol.*, 2016, **14**, 320–330.

7 J. M. Andrews, *J. Antimicrob. Chemother.*, 2001, **48 Suppl 1**, 5–16.

8 I. Wiegand, K. Hilpert and R. E. W. Hancock, *Nat. Protoc.*, 2008, **3**, 163–175.

9 I. Brook, *Rev. Infect. Dis.*, 1989, **11**, 361–368.

10 T. Artemova, Y. Gerardin, C. Dudley, N. M. Vega and J. Gore, *Mol. Syst. Biol.*, 2015, **11**, 1–11.

11 C. Tan, R. P. Smith, J. K. Srimani, K. A. Riccione, S. Prasada, M. Kuehn and L. You, *Mol. Syst. Biol.*, 2012, **8**, 617.

12 J. Karslake, J. Maltas, P. Brumm and K. B. Wood, *PLoS Comput. Biol.*, 2016, **12**, 1–21.

13 J. B. Bulitta, N. S. Ly, J. C. Yang, A. Forrest, W. J. Jusko and B. T. Tsuji, *Antimicrob. Agents Chemother.*, 2009, **53**, 46–56.

14 K. V. Singh, T. T. Tran, E. C. Nannini, V. H. Tam, C. A. Arias and B. E. Murray, *Antimicrob. Agents Chemother.*, 2017, **61**, AAC.00324-17.

15 T. S. Kaminski, O. Scheler and P. Garstecki, *Lab Chip*, 2016, **16**, 2168–2187.

16 A. R. Abate, T. Hung, R. A. Sperling, P. Mary, A. Rotem, J. J. Agresti, M. A. Weiner and D. A. Weitz, *Lab Chip*, 2013, **13**, 4864.

17 O. Scheler, N. Pacocha, P. R. Debski, A. Ruszczak, T. Kaminski and P. Garstecki, *Lab Chip*, 2017, **17**, 1980–87.

18 P. R. Debski, K. Gewartowski, M. Sulima, T. S. Kaminski and P. Garstecki, *Anal. Chem.*, 2015, **87**, 8203–8209.

19 P. R. Debski and P. Garstecki, *Biomol. Detect. Quantif.*, 2016, **10**, 24–30.

20 O. Kocaoglu and E. E. Carlson, *Antimicrob. Agents Chemother.*, 2015, **59**, 2785–2790.

21 N. G. Chorianopoulos, R. J. W. Lambert, P. N. Skandamis, E. T. Evergetis, S. A. Haroutounian and G.-J. E. Nychas, *J. Appl. Microbiol.*, 2006, **100**, 778–786.

22 R. J. W. Lambert and J. Pearson, *J. Appl. Microbiol.*, 2000, 784–790.

23 B. J. Hindson, K. D. Ness, D. a Masquelier, P. Belgrader, N. J. Heredia, A. J. Makarewicz, I. J. Bright, M. Y. Lucero, A. L. Hiddessen, T. C. Legler, T. K. Kitano, M. R. Hodel, J. F. Petersen, P. W. Wyatt, E. R. Steenblock, P. H. Shah, L. J. Bousse, C. B. Troup, J. C. Mellen, D. K. Wittmann, N. G. Erndt, T. H. Cauley, R. T. Koehler, A. P. So, S. Dube, K. a Rose, L. Montesclaros, S. Wang, D. P. Stumbo, S. P.

Hodges, S. Romine, F. P. Milanovich, H. E. White, J. F. Regan, G. a Karlin-Neumann, C. M. Hindson, S. Saxonov and B. W. Colston, *Anal. Chem.*, 2011, **83**, 8604–10.

24 M. Najah, A. D. Griffiths and M. Ryckelynck, *Anal. Chem.*, 2012, **84**, 1202–9.

25 J. L. Martinez and F. Baquero, *Antimicrob. Agents Chemother.*, 2000, **44**, 1771–1777.

26 C. Holtze, A. C. Rowat, J. J. Agresti, J. B. Hutchison, F. E. Angilè, C. H. J. Schmitz, S. Köster, H. Duan, K. J. Humphry, R. A. Scanga, J. S. Johnson, D. Pisignano and D. A. Weitz, *Lab Chip*, 2008, **8**, 1632–1639.

27 O. Scheler, T. S. Kaminski, A. Ruszczak and P. Garstecki, *ACS Appl. Mater. Interfaces*, 2016, **8**, 11318–11325.